

RESEARCH ARTICLE

Effect of Preheating on Microstructure and Mechanical Properties in Mild Steel Arc Weld Joints

Md Seam Shaikh¹, Md. Shahriar Shajib¹, Md. Abdul Kader², Dipayan Mondal¹, Md. Ashrafur Islam^{1*}

¹Department of Mechanical Engineering, Khulna University of Engineering & Technology, 9203 Khulna, Bangladesh

²Department of Mechanical Engineering, Rajshahi University of Engineering & Technology, 6204 Rajshahi, Bangladesh

ABSTRACT – Mild steel welding can result in fusion defects that affect the integrity and mechanical characteristics of welded joints. Although several techniques have been investigated to enhance the quality of the weld, it is not fully understood how preheating affects the mechanical-microstructure properties of arc-welded joints of mild steel. This study examines the effect of preheating on the mechanical characteristics and microstructure of arc-welded mild steel joints. Before welding, mild steel samples were preheated to 250°C, 450°C, and 650°C, and the welded specimens' tensile, bending, hardness, and fracture morphologies were evaluated. The results indicate that preheating significantly enhances mechanical properties, with tensile strength, ductility, and toughness increasing with temperature, particularly tensile strength, which improved by up to 35.46%. Therefore, at reduced cooling rates at 650°C, the fusion defects were improved; hence, there was better joint integrity. From the SEM analyses, a finer and homogeneous microstructure with increasing temperature also showed that the observed decrease in porosity and fusion defects corroborate the results, underlining the contribution of preheating to ensure reliability and enhanced quality of the welded mild steel joints, thereby providing useful indications on the applications of welding to industries such as automotive, aerospace, pipeline, and manufacturing machinery.

ARTICLE HISTORY

Received : 06th Sept. 2024

Revised : 12th Dec. 2024

Accepted : 20th Jan. 2025

Published : 19th Mar. 2025

KEYWORDS

Arc welding

Preheating of mild steel

SEM

Microstructure

Fusion defects

1. INTRODUCTION

Mild steel is a category of carbon steel characterized by a rather small carbon composition, typically around 0.05% to 0.25%. It is considered one of the most basic elements, possessing excellent ductility, strength, weldability, machinability, formability, and affordability. Most fast-moving industries need to join mild steel in construction, automobiles, aerospace, pipeline, and machinery production, among many more [1]. Of the different welding processes, arc welding is considered to be the simplest, most versatile, and one that can produce high-quality welds. Arc welding employs an electric arc to melt and join materials by fusion [2]. It is well known that the rapid heating and cooling cycle during welding greatly affects the surface composition and microstructure of welded joints. This process is responsible for changing phases of materials by the partial/complete dissolution of existing phases, resulting in significant microstructural alterations and chemical inhomogeneity [3]. Hot-spot stress (HSS) is generated during welding, and the size of the weld profile is a crucial part of HSS design [4]. Besides, some deforming may occur in materials due to welding, such as contraction, distortion, perforation, and irregularities in the crystal structure [5-7]. Even steels of identical strength grade may exhibit significant heterogeneities in chemical composition, resulting in diverse microstructures and mechanical properties within the Heat Affected Zone (HAZ). The mechanical characteristics of the HAZ play a pivotal role in determining the overall integrity and efficiency of welded joints [8-10]. As a result of melting and rapid heating and cooling cycles involved in the welding process, the microstructure and mechanical properties of mild steel are different from those of unwelded base metal. These are the factors that account for the loss in strength. This failure can lead to disastrous situations on structural collapse, safety hazards, economic losses, environmental damage, and loss of public confidence [11]. Such failures can result in loss of structural integrity and loss of life and property, with huge economic losses and environmental damage. It is, therefore, of utmost importance that deep research is carried out with the aim of improving the microstructure and mechanical properties of the HAZ metal while welding mild steel.

In addition, many researchers have focused on improvements to microstructures and mechanical properties of welded zones and thermomechanical effects on material structures [12-21]. Kumar and Shahi [22] studied the influence of heat input on mechanical properties and microstructures of 304 stainless steel (SS) joints obtained by GTAW and recommended low heat input for welding of AISI 304 SS by the GTAW technique. They also noted that the low heat input during welding offers better ductility and tensile strength, minimum grain coarsening, and a smaller HAZ. In the same year, Gharibshahiyan et al. [23] evaluated the effect of welding criteria and heat input on grain growth and HAZ. They observed an approximately 20.97% refinement of grain size with a 50% rise in voltage. Additionally, when the heat input was elevated by 60%, the Brinell Hardness decreased by 7.5%, and impact energy and toughness also decreased. Pirinen et al. [24] maintained a heat input range of 1.0 – 1.7 kJ mm⁻¹ while welding 8 mm HS steel and discovered that heat input in this range has minimal influence on the HAZ's impact toughness and fracture gap displacement. When

*CORRESPONDING AUTHOR | Md. Ashrafur Islam | ✉ md.islam@me.kuet.ac.bd

welding AISI 316 SS by gas tungsten arc welding, Karthick et al. [25] employed the same heat input that Kumar and Shahi [22] utilized to investigate the changes in mechanical properties and microstructures of materials. They noted that the delta ferrite content of the weld region was considerably enhanced by the addition of heat input. Further research was conducted by Kornokar et al. [26] on the influences of heat input during automatic GTAW on mechanical characteristics and microstructure of thermo-mechanically controlled processed S500MC steel. They performed autogenous mode for welding butt joints using six different heat inputs. It was found that the packet's size and amount of retained austenite increased with increasing heat input. To eliminate problems such as residual stress, cold cracking, fatigue damage, and distortion due to fusion welding HSLA steels of naval grade, Nathan et al. [27] carried out distinct welding techniques like SMAW, GMAW, and FSW. After comparing the microstructures and mechanical attributes of these welding processes, they concluded that FSW exhibited greater strength values among the three welded joints, whereas GMAW exhibited higher impact toughness and lower hardness (304 HV).

Post-weld heat treatment (PWHT) is an important method to enhance the mechanical characteristics and microstructure of the HAZ. Ahmad and Bakar [28] studied how PWHT affects the mechanical and microstructure characteristics of GMAW cold metal transfer (CMT) process welded AA6061 samples. They observed a 25.6% enhancement in hardness, a 3.8% improvement in tensile strength, and 21.5% higher elongation after PWHT due to precipitates being distributed finely and uniformly at the weld joints, narrower voids, smaller spaces between the grains, and smaller grain sizes. Yi et al. [29] examined the impact of PWHT on microstructure-mechanical characteristics of heat-treated identical alloys used by Ahmad and Bakar [28] welded through a double-pulsed MIG welding process.

Preheating the base metal is another efficient approach to minimize welding defects, as noted by Zhu et al. [30]. Luo et al. [31] investigated the employment of a preheating treatment in the aluminum alloy 5052 welding schedule to mitigate the impact of the uneven oxide film on the quality of the resistance spot weld. They suggested studying and improving all welding factors for a particular use. An exploratory analysis by He et al. [32] showed that preheating at 200°C to 250°C enhanced the thick section welding joints of 5083 Al-alloy. Zhu et al. [30] noticed a sturdy weld joint in the narrow-gap GMAW process of 5083 Al-alloy, devoid of fusion faults, obtained by preheating at 250°C and a correct oscillating arc. Ma et al. [33] applied a preheating treatment of 100°C to the brazed fusion welding of 5052 Al-alloy and obtained a sound weld joint. Rajani et al. [5] evaluated the impact of preheating at 450°C and 650°C on the GTAW 316L stainless steel and found that increasing the preheating temperature enhanced the corrosion resistance of the welded joints. Charkhi and Akbari [34] numerically and experimentally investigated the pre-heating effects on residual stresses of welded steel pipes and disclosed that the residual stresses from repair welding of pipe decrease as the pre-heating temperature increases. Jawad et al. [11] found that preheating of gas tungsten arc welded AISI 1045 medium carbon steel leads to finer grain structure. This finer grain structure is attributed to the reduction in cooling rate. Another group of researchers, Čičo et al. [35], discovered that various welding methods may have differing preheating sensitivities. Zhao et al. [36] welded magnesium alloy at seven distinct preheating temperatures using a pulsed laser welder and found that pores and solidification cracks disappear at 200°C preheating temperature. Landowski et al. [37] used different preheating temperatures and welding parameters during the welding of lean duplex stainless steel grade. Muangjunburee et al. [38] examined the effect of preheating temperatures and heat input of welding on the microstructure of weld metal and HAZ of thermite welded rail. Sun and Dilger [39] observed lower transverse residual stress for higher preheating temperatures during the study of the impact of preheating on residual stresses in ultra-high-strength steel welds.

However, based on the previous literature, it is observed that the influence of preheating on various processes is not yet clear, and its effect on arc-welded mild steel joints remains uncertain. Therefore, it is crucial to understand the mechanism by which preheating affects the weld zone to offer an effective solution for mild steel joints. To tackle this issue, a comprehensive study of mild steel joints was undertaken with arc welding and preheating treatment at varying temperatures to examine the properties of welded joints, like tensile strength, bending strength, and hardness. In addition, the tensile fracture morphologies of welded joints were analyzed through SEM to reveal the fracture mechanism.

2. METHODS AND MATERIAL

2.1 Materials

In this experimental study, mild steel plates were used as a base material for electric arc welding. The plate used in this experiment is a mild steel plate with dimensions of 4 meters in length, 0.5 meters in width, and 0.005 meters in thickness. The composition of the mild steel plate contains 0.25% to 0.29% carbon and about 98% iron, having an Ultimate Tensile Strength of 400 to 550 MPa and a Yield Strength of 250 MPa [40]. The plate was then CNC-machined into the required quantity of samples 100 mm x 10 mm x 5 mm in dimension. Then, the samples were carefully cleaned by maintaining the operations in sequences: cleaning with acetone, followed by immersion in a 5% sodium hydroxide solution at 50-60°C for 5 minutes, then soaking in 30% nitric acid for less than 1 minute, rinsing with water at 50-60°C, and finally drying at 100°C in an electric oven. After that, the cleaned samples were preheated using an electric muffle furnace at a controlled heating rate of 10°C per minute. The samples were kept in the furnace at the highest temperature of 250°C, 450°C, and 650°C for 30 minutes to prepare three different batches of heat-treated samples.

2.2 Welding Process

The plates were welded at a lower temperature than the furnace set temperature after removal from the furnace. The temperature of the plate was decreased through natural cooling in the atmosphere. This experiment used the arc welding method with an alternating current of 220V and 50Hz. Since the preheated materials were being welded, a thermocouple was used to measure the exact temperature during the welding process. The recorded temperature is listed in Table 1. The welding speed was kept constant during the welding process. The two inclined parts were placed face to face, forming a V shape. Then, these two materials were connected through arc welding. The length of the V groove was 20 mm, and this groove was welded. Thus, the welded track length was 20 mm for each sample. Both the upper and lower surfaces were welded. For welding, ESAB Ferrospeed rutile-coated electrodes (AWS A5.1: E 6012, IS: 814 ER 4124) of 4 mm diameter were used. The welding current was set to 100 A to match the diameter of the electrode and thickness of the mild steel plate for achieving a consistent, smooth weld bead. Unwelded and welded plates are shown in Figure 1. Following welding, the plates were allowed to cool naturally in the ambient atmosphere, which was at a temperature of 32°C on the day of the experiment. For each mechanical test, three samples were welded using one set of parameters, resulting in a total of 36 samples.

Table 1. Recorded temperature

Sample No.	Temperature (°C)	
	Preheating	During Welding
1-9	-	Room
10-18	250	100
19-27	450	200
28-36	650	300



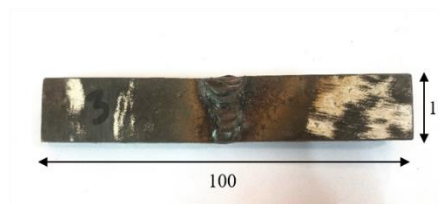
(a) Mild Steel Plate



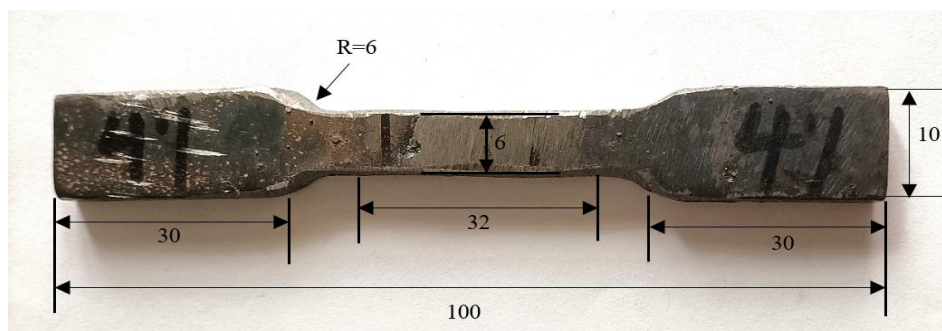
(b) CNC Milling



(c) Cut Plate



(d) Welded Bending Test Sample



(e) Welded Tensile Test Sample

Figure 1. (a) Collected mild steel plate, (b) CNC milling operation, (c) Cut plate (d) Prepared bending test sample, and (e) Prepared tensile test sample (All the dimensions are in millimeters)

2.3 Mechanical Testing

The tensile test samples were prepared according to the ASTM E8/E8M method [41]. Bending tests were conducted according to ASTM E190 standard [42]. These tests were conducted using a Shimadzu Universal Testing Machine (AGX V 300KN). The photographs of prepared samples, along with detailed dimensions, are presented in Figure 1(d) and Figure 1(e). The center parts of the welded zone were cut from the welded sample for Vickers Hardness tests. The Vickers hardness test involved pressing a pyramidal diamond-shaped indenter into the surface of the welded zone under a known load [43]. At least three samples were tested for each set of parameters to ensure statistical validity.

2.4 SEM Imaging

An SEM is utilized to observe high magnification/resolution surface morphology and microstructure in materials of different types. In treating the samples by metallography for observation in an SEM, the sample preparation involved the cutting of the small pieces of samples by the use of a disc grinder. Samples were then kept in an electric heater at 40°C for 24 hours to remove impurities/moisture from the surface of the samples. It carefully cleaned the specimens with isopropyl alcohol to remove adhering material that was left from cutting and followed with drying of the samples afterward. The samples were fixed onto the double-sided adhesive carbon tape of an SEM specimen holder. The metallization of conductive material as a thin coat, like that of gold or similar metals, was conducted in order to allow conductivity when taking images of the SEM chambers for micro-structural examination purposes. Scanning electron microscopic studies were done in the Modern Equipment & Research Centre (MERC) of Khulna University of Engineering & Technology, Bangladesh, using a Jeol Scanning Electron Microscope - JCM7000NeoScope™ Benchtop SEM.

3. RESULTS AND DISCUSSION

3.1 Tensile Test Result

Tensile tests were performed to investigate preheating effects on the mechanical properties of the welded sample. The stress-strain responses of the welded samples preheated at 250°C, 450°C, and 650°C are presented in Figure 2. This figure also presents the stress-strain response of a welded sample without any preheating for comparison. It is observed that the ultimate strength increases with the increase of preheating temperature. This is possible because of the reduction of fusion defects in the welded joint due to preheating the base metal. However, the rate of strength enhancement with temperature decreases beyond 450°C preheating temperature, as observed in Figure 3.

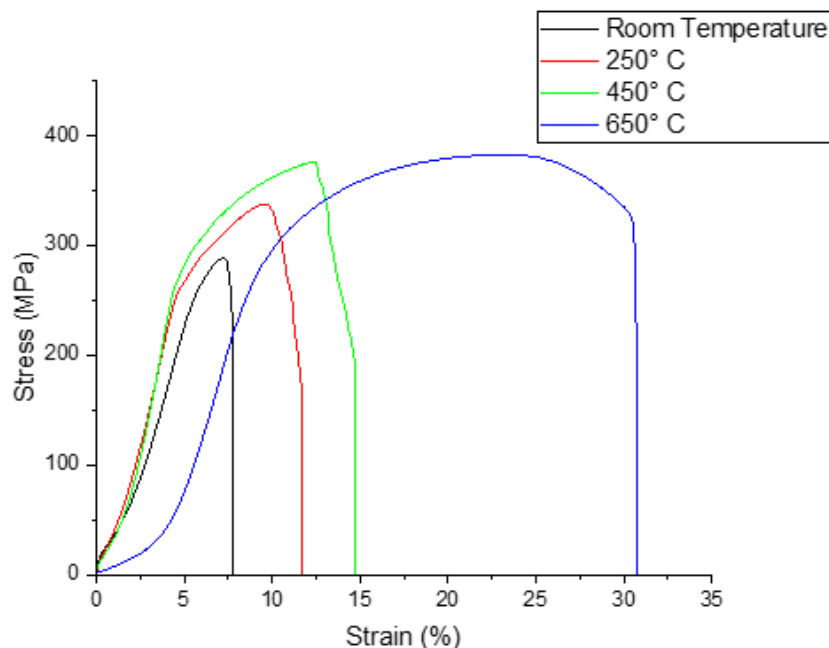


Figure 2. Stress-strain responses of the welded specimen at room temperature and three different preheated temperatures

Also, it is evident from Figure 2 that with the increase in preheated temperature, the ductility of the welded joint increases. It is calculated that the strain increases by 70% for preheating the welded joint from room temperature to 250°C. The maximum strain increase of 325% was found for the sample preheated at a temperature of 650°C.

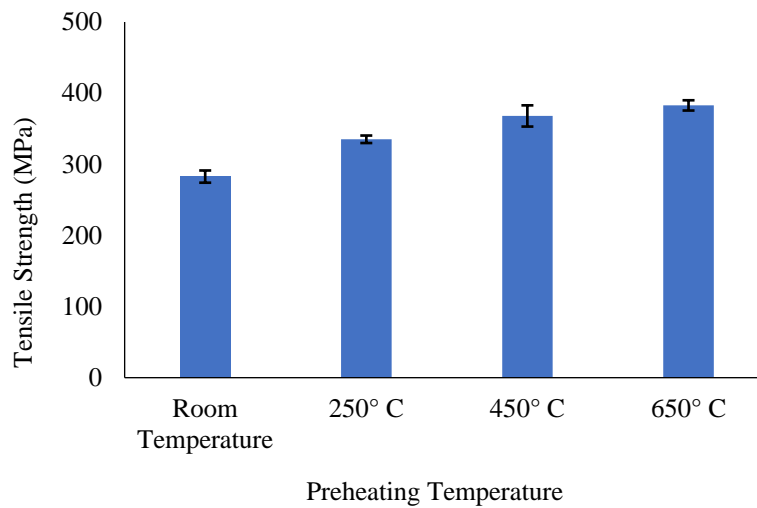


Figure 3. Variation of tensile strength with preheating temperature

Figure 4 demonstrates that the highest modulus of elasticity is found at a 250°C preheating temperature. This is because the fusion defects are reduced due to preheating the base metal. However, the rigidity of the joints increases beyond 250°C. Thus, the elastic modulus decreased beyond 450°C preheating temperatures. The reasons behind this variation of modulus of elasticity were extensively analyzed using SEM images, which will be discussed in subsequent sections.

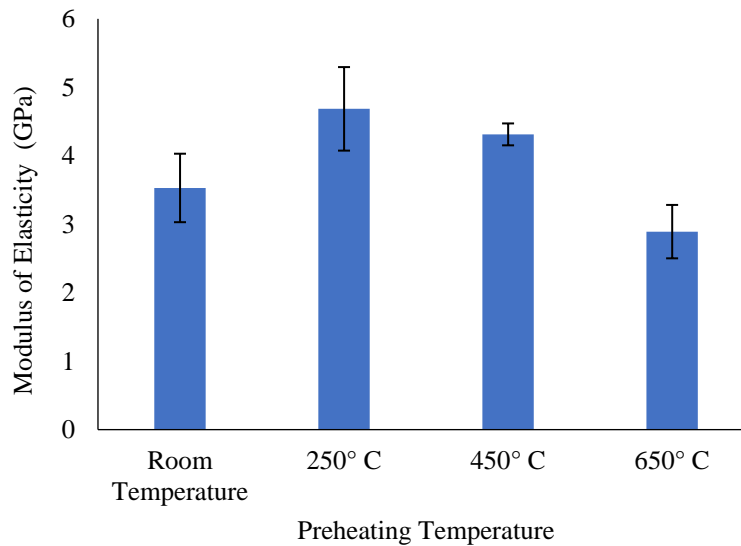


Figure 4. Obtained modulus of elasticity at elevated preheating temperature

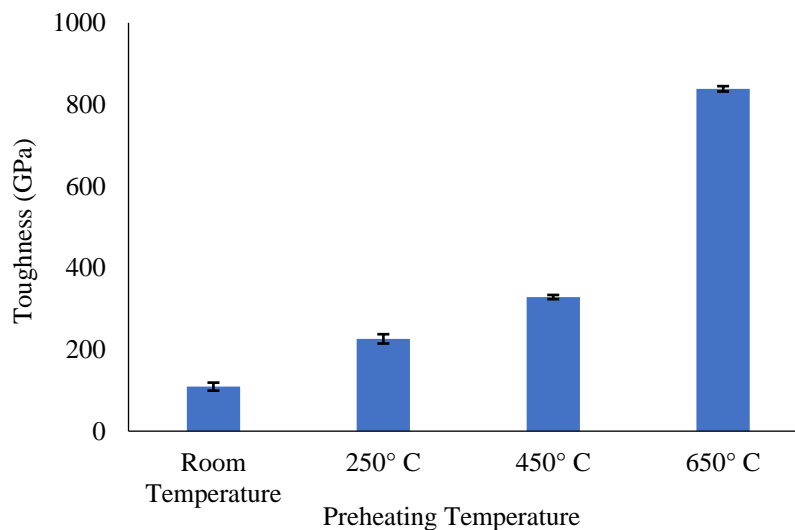


Figure 5. Obtained toughness at elevated preheating temperature

Figure 5 shows the toughness obtained at elevated preheating temperatures. The area under the stress versus strain graph indicates the toughness. It is found that the area under the curve increases as we increase the preheating temperature, without exception. Therefore, it can be said that by increasing the preheating temperature, its toughness increases. We get the highest toughness at a preheating temperature of 650°C, as shown in Figure 5. It is further implied that the joint is stronger for the welding joint at a higher preheating temperature. This also means that the fusion defect is minimal at higher-temperature welding. This is further verified by the SEM microstructure of the welding joints at high temperatures.

3.2 Bending Test Result

The bending tests of the welded joint specimens are also carried out using the same UTM. Figure 6 shows the average test results of the bending test results for various preheating conditions. It is noted that the specimen preheated at 650°C needed the highest force to start breaking. However, the displacement is less than that of the specimen preheated at 450°C. By increasing the preheating temperature, the amount of force needed to break during the bending test increases without any exception. This is because the joint becomes stronger by reducing fusion defects, which, in this case, occurs when preheated. This is also why the sample preheated at 650°C has the highest maximum bending strength seen from the bar chart (Figure 7).

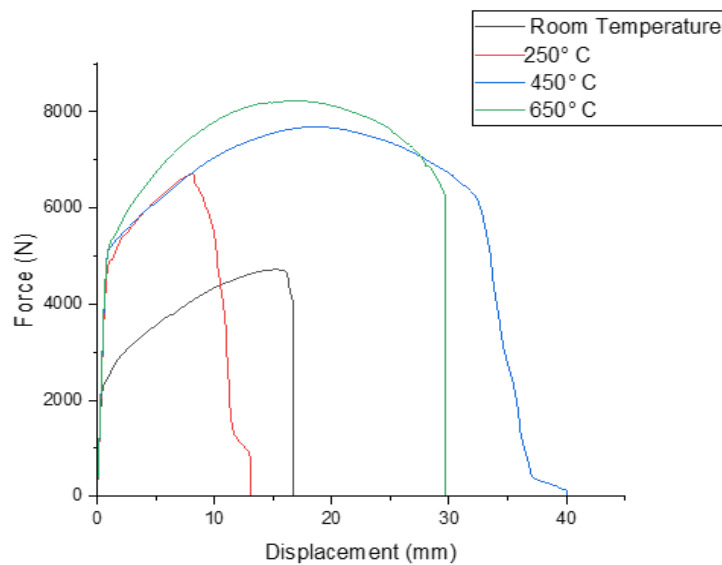


Figure 6. Force vs. displacement graph for bending test

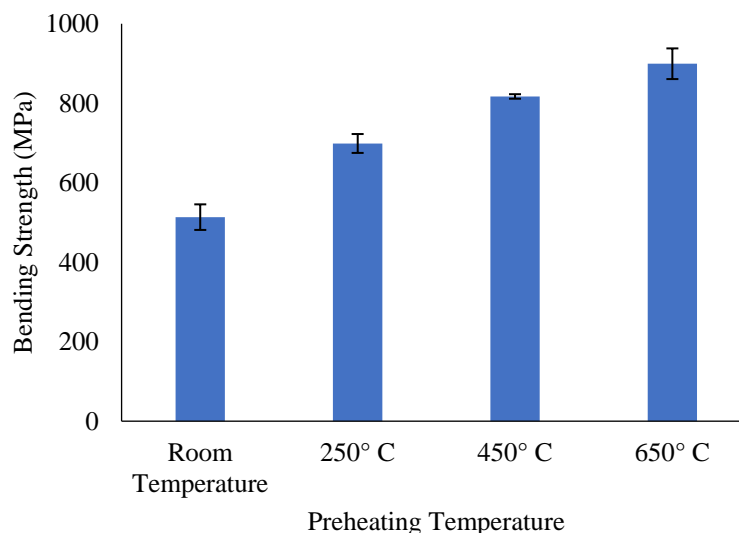


Figure 7. Bending strength obtained at elevated preheating temperature

The energy absorption capacity during the deformation of the specimens is also assessed. Figure 8 shows the energy absorption obtained at different elevated preheating temperatures. The area under the force vs. displacement graph indicates the energy absorption. The energy absorption is highest when the specimens are preheated at 450°C. From room temperature to 450°C preheating temperature, the energy absorption increases without any exception. But after that, it reduced by 15% for the temperature of 650°C. We have already discussed that their fusion defect reduces so much when

the specimens are preheated at 650°C, and the weld joint becomes stronger and more rigid. So, it requires a higher force to be bent or deformed. However, since it is more rigid, it gets less bent than the specimens preheated at 450°C.

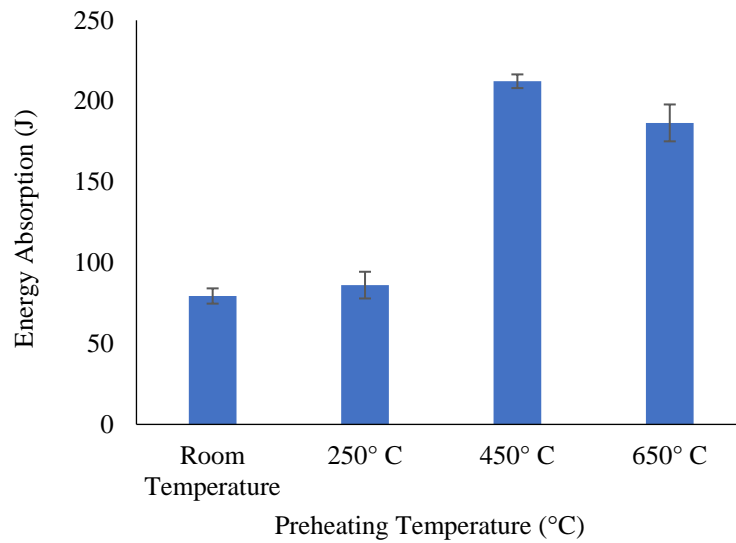


Figure 8. Energy absorption obtained at elevated preheating temperature

3.3 Hardness Test Result

It is observed from Figure 9 that the difference in hardness between the welding zone and the heat-affected area reduces as the preheating temperature starts to increase. Preheating here helps reduce hardness gradients between the weld and heat-affected zones by promoting slower cooling rates, resulting in more uniform mechanical properties throughout the welded joint.

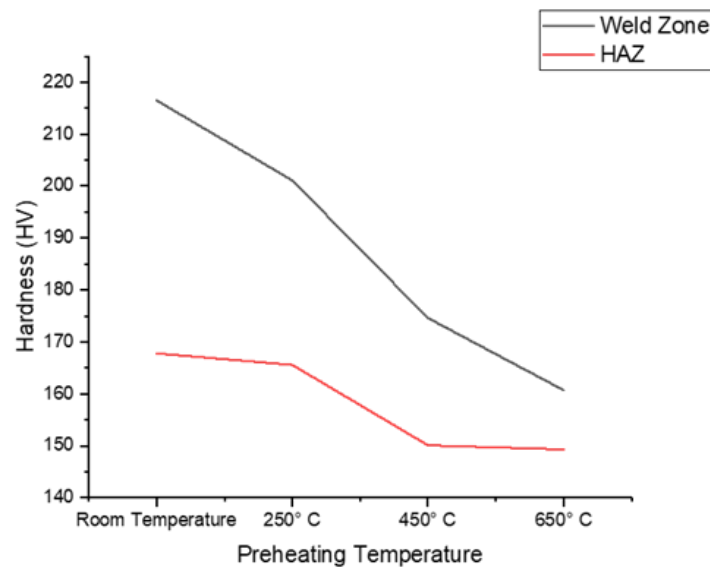


Figure 9. Variation of hardness at elevated preheating temperature of weld zone and HAZ

3.4 SEM Analysis

3.4.1 Samples Without Preheating

Here, from SEM images, for the sample at room temperature (without preheating), we observed irregular dimples on the fractured surface, which are shown in Figure 10(a), Figure 10(b), Figure 10(c), and Figure 10(d). These figures show that a fracture occurred at the open side of V, followed by a huge crack path where a greater fusion defect occurred, which reduced the tensile strength of the sample. Zhu et al. [30] also found fusion defects at low preheating temperatures in a similar manner.

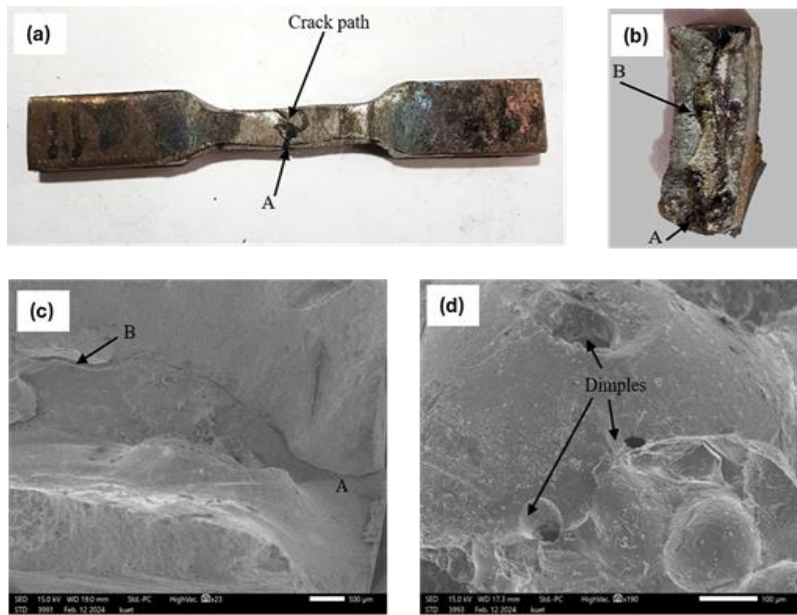


Figure 10. Sample without preheating: (a) Fractured sample, (b) SEM specimen, (c) and (d) SEM images

3.4.2 Preheated at 250°C

At a preheated temperature of 250°C, from SEM images of Figure 11(c) and Figure 11(d), it is seen that lack of fusion between weld metal and base metal had become a source of cracking, which caused the samples to be fractured rapidly with little stress and strain. Like the previous one, the fracture initially occurred at the open side of the V shape and followed a path along the fusion defect. Large and small pores were also found on the fracture surface. Near the fusion defect region, a high content of oxygen was present, as shown in the EDS of the sample (Figure 12), which may contribute to the formation of pores.

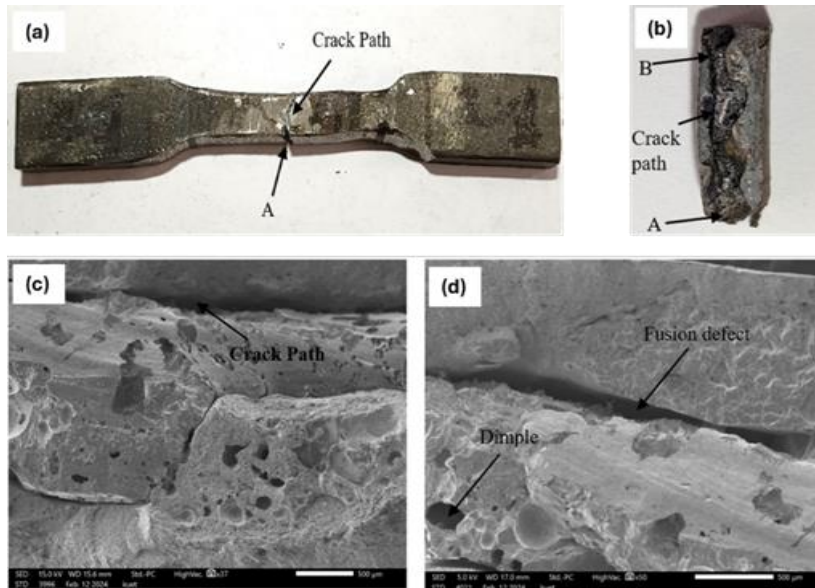


Figure 11. Preheated at 250°C: (a) Fractured sample, (b) SEM specimen, (c) and (d) SEM images indicating the major modes of failure of a specimen

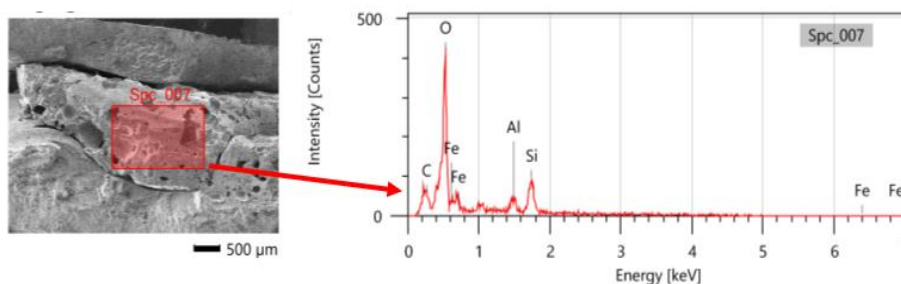


Figure 12. EDS of the specimen preheated at 250°C

3.4.3 Preheated at 450°C

Like the previous two samples, the fracture also initiates at the open side of V. Here, the fusion defect is considerable at this point. However, the fusion defect was overall reduced from the previous two preheating temperatures. Also, the crack path became narrow, as observed in Figure 13(d) and Figure 13(e). Here, we observed good quality of weld joint due to finer dimples and less fusion defect into the crack path. Preheating at this temperature slowed down the cooling rates, which allowed for the formation of a finer, more homogeneous microstructure that improved the mechanical properties of the welded sample. The portion indicated by C in Figure 13(b) and Figure 13(f) didn't form any crack; it was a very nicely welded joint. Furthermore, the joint was just torn apart without forming any more cracks along the crack paths. So, this specimen preheated at 450°C exhibits better tensile strength and toughness than the previous two conditions.

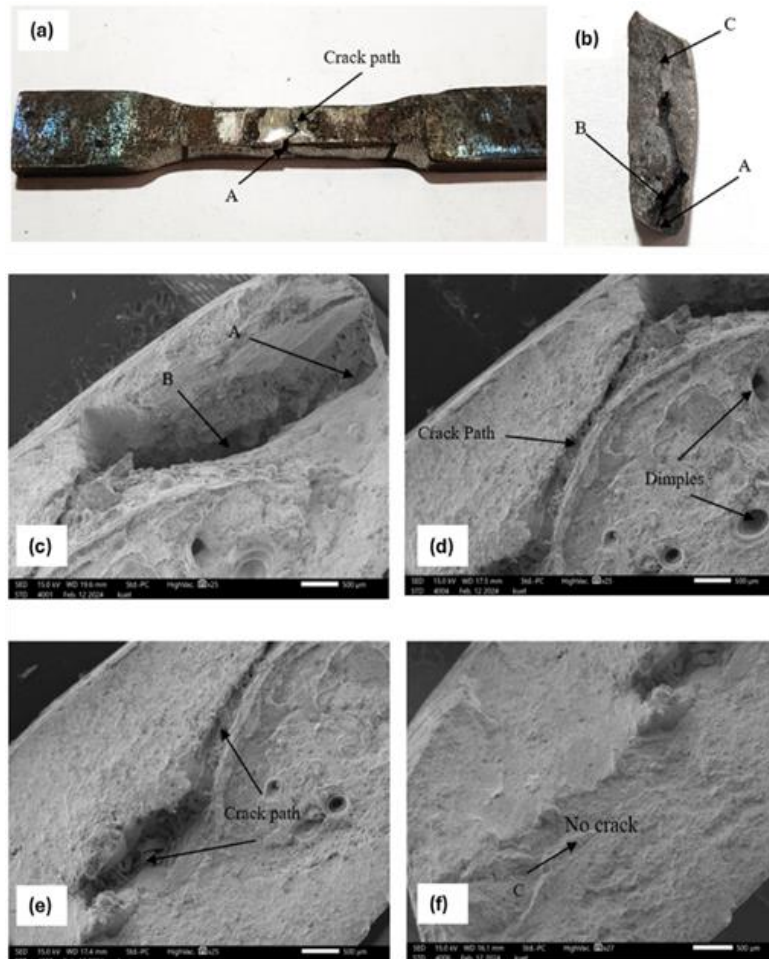


Figure 13. Preheated at 450°C: (a) Fractured sample, (b) SEM specimen, (c), (d), (e) and (f) SEM images

3.4.4 Preheated at 650°C

At this highly preheated specimen, fusion defects were found less compared to all other samples mentioned above. The fusion defect is reduced at this high preheated temperature due to a more gradual cooling process, which allows uniform solidification of the weld zone as a result of reduced temperature gradient between the weld zone and surrounding material. Similar findings were presented by Yuan et al. [44] in their study of the effects of preheating on the residual stress distribution and deformation of a Q345C steel butt-welded joint. Furthermore, moisture was evaporated before welding started, which resulted in a reduction of hydrogen-induced cracking. A crack is observed in Figure 14(b) in the middle portion of the V groove, which is a noticeable change from the previous samples. This crack, however, appears to be superficial and has no substantial effect on the weld's tensile strength or ductility, as there is no visible crack route in the sample. Instead, an indentation resembling a crack is visible, as shown by B in Figures 14(e) and 14(f). In this sample, the reduction of pores is observed, which indicates the reduction in porosity. At this higher temperature, the change in strength is not that much. This is because the small and scattered pores have minimal impact on the tensile strength. Dimples on the fractured surface of this sample are smaller and shallower but of high density, which formed during plastic deformation, which directly correlates with the ductile failure observed in the tensile test results. It is evident from the mechanical and microstructure evolution of preheated welded samples that the higher the preheating temperature, the better the microstructure and tensile strength. Preheating at this temperature also results in lower hardness gradients between the weld zone and HAZ of the welded mild steels.

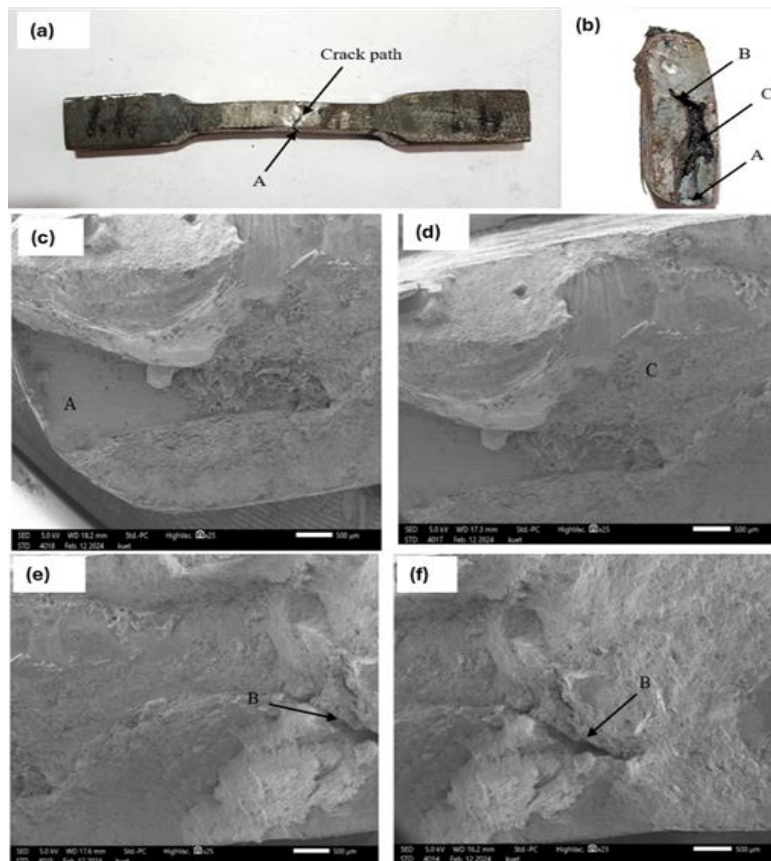


Figure 14. Preheated at 650°C: (a) Fractured sample, (b) SEM specimen, (c), (d), (e) and (f) SEM images

The results of this study demonstrate an increase in tensile strength, ductility, and toughness, particularly at 450°C and 650°C preheating temperatures, as well as improvement of the microstructure of arc-welded mild steel joints. These enhancements result from fewer fusion defects, less porosity, and the development of a finer, more uniform microstructure, as evidenced through SEM examination. Preheating also reduces temperature gradients between the welding zone and HAZ. Other works also reported such an improvement in the quality of welds with preheating. In fact, the works of Jawad et al. [11] and Zhu et al. [30] reported that preheating increases the strength of welds and reduces defects.

Preheating at higher temperatures can lead to better quality welds for industries such as aerospace and automotive, reducing the possibility of failure in critical applications. The results of this work contribute to the theoretical understanding of preheating treatment with respect to weld microstructure and stability, besides its industrial importance. There are certain limitations regarding the research. It was related only to preheating; the effects of other welding parameters were not studied concerning the quality of the weld. Long-term performance and residual stresses also need consideration. These should be examined in subsequent research. Despite those drawbacks, the strong points that support this study are the wide-ranging examination of various preheating temperatures and the use of tensile, bending, and SEM analyses to correlate preheating with weld quality. This research provides valuable information for the optimization of welding processes in the industry.

4. CONCLUSIONS

The present study represents an essential role of preheating in the improvement of mechanical and microstructural aspects in arc-welded joints of mild steel. The major findings are as follows:

- **Tensile Strength and Ductility:** Preheating enhanced tensile strength and ductility, with the most significant improvements occurring up to 450°C. Preheating at 650°C developed better joint integrity due to consistent solidification of the weld zone.
- **Durability and Energy Absorption:** Preheated samples demonstrated enhanced toughness, peaking at 650°C due to fewer fusion defects and a more ductile failure mechanism.
- **Hardness Distribution:** The preheating process reduced hardness gradients between the weld zone and HAZ, resulting in a more uniform joint.
- **Microstructure Evaluation:** SEM examinations showed that porosity and sites of fracture initiation decreased along with fusion defects by increasing preheating temperatures. Finer dimples, along with a microstructural uniformity, are observed under the conditions at high preheating temperatures.

The experimental test results showed that preheating treatment improves weld quality and mechanical performance in mild steel joints. While 450°C is optimal for strength, ductility, and toughness, 650°C reduces fusion defects and improves the integrity of the joint. The present work could provide a better background to enhance the preheating parameters for industrial applications.

CONFLICT OF INTEREST

The authors declare no conflict of interest regarding the publication of this work, and no significant financial support was received for this work that could have influenced its outcome. We assure that the manuscript has been read and approved for submission by all the named authors.

AUTHORS CONTRIBUTION

M.S. Shaikh (Conceptualization; Methodology; Investigation; Data curation; Analysis; Writing - original draft; Writing - review & editing; Visualization; Validation)

M.S. Shajib (Conceptualization; Methodology; Investigation; Data curation; Analysis; Writing - original draft)

M.A. Kader (Writing - review & editing)

D. Mondal (Writing - review & editing)

M.A. Islam (Conceptualization; Methodology; Writing - review & editing; Discussion; Supervising)

ACKNOWLEDGEMENTS

The authors greatly acknowledge the experimental facilities provided by the Department of Mechanical Engineering, Khulna University of Engineering and Technology.

REFERENCES

- [1] E. Osarolube, I. Owate, and N. Oforka, "Corrosion behaviour of mild and high carbon steels in various acidic media," *Scientific Research and Essay*, vol. 3, no. 6, pp. 224-228, 2008.
- [2] A. B. Murphy, "A perspective on arc welding research: the importance of the arc, unresolved questions and future directions," *Plasma Chemistry and Plasma Processing*, vol. 35, no. 3, pp. 471-489, 2015.
- [3] H. Conrad, "Effects of electric current on solid state phase transformations in metals," *Materials Science and Engineering: A*, vol. 287, no. 2, pp. 227-237, 2000/08/15/ 2000.
- [4] E. Zavvar, P. Rosa-Santos, E. Ghafoori, and F. Taveira-Pinto, "Analysis of tubular joints in marine structures: A comprehensive review," *Marine Structures*, vol. 99, p. 103702, 2025.
- [5] H. Z. Rajani, H. Torkamani, M. Sharbati, and S. Raygan, "Corrosion resistance improvement in gas tungsten arc welded 316L stainless steel joints through controlled preheat treatment," *Materials & Design*, vol. 34, pp. 51-57, 2012.
- [6] U. Soy, O. Iyibilgin, F. Findik, C. Oz, and Y. Kiyan, "Determination of welding parameters for shielded metal arc welding," *Scientific Research and Essays*, vol. 6, no. 15, pp. 3153-3160, 2011.
- [7] F. Uzun and A. N. Bilge, "Application of ultrasonic waves in measurement of hardness of welded carbon steels," *Defence Technology*, vol. 11, no. 3, pp. 255-261, 2015.
- [8] M. Hamada, Y. Fukada, and Y.-i. Komizo, "Microstructure and precipitation behavior in heat affected zone of C-Mn microalloyed steel containing Nb, V and Ti," *Iron and Steel Institute of Japan International*, vol. 35, no. 10, pp. 1196-1202, 1995.
- [9] C. Davis and J. King, "Cleavage initiation in the intercritically reheated coarse-grained heat-affected zone: Part I. Fractographic evidence," *Metallurgical and Materials Transactions A*, vol. 25, pp. 563-573, 1994.
- [10] A. Lambert-Perlade, A.-F. Gourgues, and A. Pineau, "Austenite to bainite phase transformation in the heat-affected zone of a high strength low alloy steel," *Acta Materialia*, vol. 52, no. 8, pp. 2337-2348, 2004.
- [11] M. Jawad, M. Jahanzaib, M. A. Ali, M. U. Farooq, N. A. Mufti, C. I. Pruncu et al., "Revealing the microstructure and mechanical attributes of pre-heated conditions for gas tungsten arc welded AISI 1045 steel joints," *International Journal of Pressure Vessels and Piping*, vol. 192, p. 104440, 2021.
- [12] P. Das, A. Benslimane, M. Islam, D. Mondal, and M. J. H. Nazim, "A thermo-mechanically loaded rotating FGM cylindrical pressure vessels under parabolic changing properties: An analytical and numerical analysis," *Heliyon*, vol. 10, no. 4, e25969, 2024.
- [13] P. Das, M. Islam, S. Somadder, and M. J. A. O. A. M. Hasib, "Analytical and numerical solutions of pressurized thick-walled FGM spheres," *Archive of Applied Mechanics*, vol. 93, no. 7, pp. 2781-2792, 2023.
- [14] M. Hasan, M. A. Islam, Z. Huang, J. Zhao, and Z. J. M. S. Jiang, "Influence of sintering time on diffusion bonding of WC-10Co and AISI4340 by spark plasma sintering," *Materials Science and Technology*, vol. 39, no. 6, pp. 683-693, 2023.
- [15] E. Zavvar, F. Taveira-Pinto, and P. Rosa-Santos, "Identification of probability distributions of SCFs in three-planar KT-joints," *Ocean Engineering*, vol. 312, p. 119222, 2024.

- [16] E. Zavvar, A. G. Majidi, P. R. Santos, and F. Taveira-Pinto, "Optimal probability distribution for SCF_{max} in KT-joints strengthened with concrete in wind turbine support structures," *Journal of Constructional Steel Research*, vol. 222, p. 108994, 2024.
- [17] E. Zavvar, F. Sousa, G. Giannini, F. Taveira-Pinto, and P. R. Santos, "Probability of maximum values of stress concentration factors in tubular DKT-joints reinforced with FRP under axial loads," in *Structures: Elsevier*, vol. 66 p. 106809, 2024.
- [18] E. Zavvar, G. Giannini, F. Taveira-Pinto, and P. R. Santos, "Parametric study of stress concentration factors in KT connections reinforced with concrete subjected to axial loads," *Ocean Engineering*, vol. 298, p. 117209, 2024.
- [19] E. Zavvar, J. Henneberg, and C. G. Soares, "Stress concentration factors in FRP-reinforced tubular DKT joints under axial loads," *Marine Structures*, vol. 90, p. 103429, 2023.
- [20] E. Zavvar and C. G. Soares, "Stress distribution in uniplanar KT joints reinforced with fibre reinforced polymer subjected to the axial loadings," in *Advances in the Analysis and Design of Marine Structures: CRC Press*, pp. 565-575, 2023.
- [21] E. Zavvar, H. S. Abdelwahab, E. Uzunoglu, B.-Q. Chen, and C. Guedes Soares, "Stress distribution on the preliminary structural design of the CENTEC-TLP under still water and wave-induced loads," *Journal of Marine Science and Engineering*, vol. 11, no. 5, p. 951, 2023.
- [22] S. Kumar and A. Shahi, "Effect of heat input on the microstructure and mechanical properties of gas tungsten arc welded AISI 304 stainless steel joints," *Materials & Design*, vol. 32, no. 6, pp. 3617-3623, 2011.
- [23] E. Gharibshahiyan, A. H. Raouf, N. Parvin, and M. Rahimian, "The effect of microstructure on hardness and toughness of low carbon welded steel using inert gas welding," *Materials & Design*, vol. 32, no. 4, pp. 2042-2048, 2011.
- [24] M. Pirinen, Y. Martikainen, P. Layus, V. Karkhin, and S. Y. Ivanov, "Effect of heat input on the mechanical properties of welded joints in high-strength steels," *Welding International*, vol. 30, no. 2, pp. 129-132, 2016.
- [25] B. Karthick, L. Shrihari, M. Sakthivel, S. Shriram, and V. Silambarasan, "Effect of heat input on the microstructure and mechanical properties of gas tungsten arc welded AISI 316 stainless steel joints," *International Research Journal on Advanced Science Hub*, vol. 2, no. 08, pp. 23-27, 2020.
- [26] K. Kornokar, F. Nematzadeh, H. Mostaan, A. Sadeghian, M. Moradi, D. G. Waugh et al., "Influence of heat input on microstructure and mechanical properties of gas tungsten arc welded HSLA S500MC steel joints," vol. 12, no. 4, p. 565, 2022.
- [27] S. R. Nathan, V. Balasubramanian, S. Malarvizhi, and A. Rao, "Effect of welding processes on mechanical and microstructural characteristics of high strength low alloy naval grade steel joints," *Defence Technology*, vol. 11, no. 3, pp. 308-317, 2015.
- [28] R. Ahmad and M. Bakar, "Effect of a post-weld heat treatment on the mechanical and microstructure properties of AA6061 joints welded by the gas metal arc welding cold metal transfer method," *Materials & Design*, vol. 32, no. 10, pp. 5120-5126, 2011.
- [29] J. Yi, G. Wang, S. Li, Z. Liu, and Y. Gong, "Effect of post-weld heat treatment on microstructure and mechanical properties of welded joints of 6061-T6 aluminum alloy," *Transactions of Nonferrous Metals Society of China*, vol. 29, no. 10, pp. 2035-2046, 2019.
- [30] C. Zhu, X. Tang, Y. He, F. Lu, and H. Cui, "Effect of preheating on the defects and microstructure in NG-GMA welding of 5083 Al-alloy," *Journal of Materials Processing Technology*, vol. 251, pp. 214-224, 2018/01/01/ 2018.
- [31] Z. Luo, S. Ao, Y. J. Chao, X. Cui, Y. Li, and Y. Lin, "Application of pre-heating to improve the consistency and quality in AA5052 resistance spot welding," *Journal of Materials Engineering and Performance*, vol. 24, pp. 3881-3891, 2015.
- [32] Y. He, X. Tang, C. Zhu, F. Lu, and H. Cui, "Study on insufficient fusion of NG-GMAW for 5083 Al alloy," *The International Journal of Advanced Manufacturing Technology*, vol. 92, pp. 4303-4313, 2017.
- [33] H. Ma, G. Qin, L. Wang, X. Meng, and L. Chen, "Effects of preheat treatment on microstructure evolution and properties of brazed-fusion welded joint of aluminum alloy to steel," *Materials & Design*, vol. 90, pp. 330-339, 2016.
- [34] M. Charkhi and D. Akbari, "Experimental and numerical investigation of the effects of the pre-heating in the modification of residual stresses in the repair welding process," *International Journal of Pressure Vessels and Piping*, vol. 171, pp. 79-91, 2019.
- [35] P. Čičo, D. Kalincová, and M. Kotus, "Influence of welding method on microstructural creation of welded joints," *Research in Agricultural Engineering*, vol. 57, no. Special Issue, pp. S50-S56, 2011.
- [36] P. Zhao, X. Zhang, S. Bian, W. Zhang, and Z. Cao, "Effect of preheating temperature on the defects in pulsed laser welding of sheet AZ31 magnesium alloy," *Materials Letters*, vol. 355, 2024.
- [37] M. Landowski, S. C. Simon, C. Breznay, D. Fydrych, and B. Varbai, "Effects of preheating on laser beam-welded NSSC 2120 lean duplex steel," *The International Journal of Advanced Manufacturing Technology*, vol. 130, no. 3, pp. 2009-2021, 2024.
- [38] P. Muangjunburee, H. Z. Oo, S. Z. Abd Rahim, and B. Srikarun, "Effects of heat input and preheating temperature on the microstructure and hardness of repairing the heat-affected zone of thermite welded rail head surface," *Indonesian Journal of Science and Technology*, vol. 9, no. 2, pp. 421-440, 2024.
- [39] J. Sun and K. Dilger, "Influence of preheating on residual stresses in ultra-high strength steel welded components," *Journal of Materials Research and Technology*, vol. 25, pp. 3120-3136, 2023.
- [40] S. Rajkumar, M. Lijalem, T. Aklilu, and V. Mohanavel, "Prediction and estimation of electroplating characteristics, corrosion rate of zinc coated mild steel coupling," *Carbon*, vol. 100, pp. 0.25-0.290.
- [41] M. Cayard and W. Bradley, "A comparison of several analytical techniques for calculating JR curves from load-displacement data and their relation to specimen geometry," *Engineering Fracture Mechanics*, vol. 33, no. 1, pp. 121-132, 1989.

- [42] S. Vaynman, M. E. Fine, and C. Hahin, *Formability of New High Performance A710 Grade 50 Structural Steel*, Illinois Center for Transportation Series No. 14-002, 2014.
- [43] J.-M. Schneider, M. Bigerelle, and A. Iost, "Statistical analysis of the Vickers hardness," *Materials Science and Engineering: A*, vol. 262, no. 1-2, pp. 256-263, 1999.
- [44] J. Yuan, H. Ji, Y. Zhong, G. Cui, L. Xu, and X. Wang, "Effects of different pre-heating welding methods on the temperature field, residual stress and deformation of a Q345C steel butt-welded joint," *Materials*, vol. 16, no. 13, p. 4782, 2023.